Dalton Transactions

RSC Publishing

PAPER

View Article Online
View Journal | View Issue

Crystal structures and stability of trigonal $KLnF_4$ fluorides (Ln = Y, Ho, Er, Tm, Yb)†

Cite this: *Dalton Trans.*, 2013, **42**, 441

Andrzej Grzechnik,*[a] Nicholas Khaidukov[b] and Karen Friese[c]

Received 4th September 2012,
Accepted 1st October 2012

DOI: 10.1039/c2dt31483e

www.rsc.org/dalton

Crystal structures of pure and doped $KLnF_4$ (Ln = Y, Ho, Er, Tm, Yb) grown hydrothermally were studied with synchrotron single-crystal and powder diffraction as a function of temperature and pressure. At atmospheric conditions, $KHoF_4$ and $KErF_4$ crystallize in space group $P3_1$, while $KTmF_4$, Er:$KYbF_4$, and KYF_4 crystallize in space group $P3_2$. In both enantiomorphic structures, the K^+ and Ln^{3+} cations are completely ordered. The pseudo-symmetry of the structures with respect to the two minimal supergroups $k = 3$ ($P3_1$ and $P3_2$) and $t = 2$ ($P3_112$ and $P3_212$) increases with decreasing radius of the Ln^{3+} cation, respectively. No phase transition is detected in KYF_4 at low temperatures down to 100 K at atmospheric pressure. Er:$KYbF_4$ and KYF_4 undergo irreversible pressure-induced phase transitions at about 4 GPa. In each case, the single crystals become fragmented into several crystallites as observed during single-crystal measurements in diamond anvil cells. Up to the phase transitions, both Er:$KYbF_4$ and KYF_4 are more compressible along the *c* axis and their bulk compressibility predominantly results from the contraction of the KF_8 polyhedra. The application of pressure does not affect the distribution of the cations in the crystal structures of Er:$KYbF_4$ and KYF_4 up to the phase transitions at about 4 GPa.

Downloaded by Forschungszentrum Julich GmbH on 08/05/2013 08:19:34.
Published on 19 October 2012 on http://pubs.rsc.org | doi:10.1039/C2DT31483E

Introduction

The crystal structure of KYF_4 has been previously described in space group $P3_1$ ($a \approx 14.1$ Å, $c \approx 10.1$ Å) as a fluorite related superstructure, where the lattice of KYF_4 and the cubic face-centred lattice of fluorite (space group $Fm\bar{3}m$) are related according to $a_{trigonal} \approx \sqrt{3}$ ($\sqrt{2}\ a_{cubic}$) and $c_{trigonal} \approx \sqrt{3}\ a_{cubic}$.[1–4] The cations in KYF_4 are distributed in three layers perpendicular to the *c* axis. Within the layers, chains of Y_2F_{12} groups formed by two [YF_7] pentagonal bipyramids alternate with chains of edge-shared distorted [KF_8] cubes.

Zachariasen reported that $KLaF_4$ and $KCeF_4$, prepared by rapid precipitation from solution, have the fluorite structure (space group $Fm\bar{3}m$, $a \approx 5.9$ Å),[5,6] while the β$_1$-$KLaF_4$ and β$_1$-$KCeF_4$ materials crystallized from melts are hexagonal (space group $P\bar{6}2m$, $a \approx 6.5$ Å, $c \approx 3.8$ Å).[6,7] In the former, the K and rare earth atoms are completely disordered, while in the latter, they are partially ordered. More recently, the structures of β-$KCeF_4$ [8] and β-$KPrF_4$ [9] (both crystallized from melts) were determined to be orthorhombic (space group *Pnma*, $a \approx 6.3$ Å, $b \approx 3.8$ Å, $c \approx 15.6$ Å). Their layered structure, with a complete order of the cations, is built of distorted tricapped triangular prisms around the rare earth atoms and monocapped trigonal prisms around the K atoms.

KYF_4 and some of $KLnF_4$ (Ln = rare earth) could be prepared as nanomaterials in the cubic form by various synthesis routes at low temperatures.[10–18] During the heat treatment at atmospheric pressure, nanometric $KGdF_4$ undergoes a sequence of phase transitions cubic → orthorhombic → trigonal.[10,11] The transformations are not complete and the cubic phase is always present. On the other hand, the orthorhombic phases of bulk $KCeF_4$ [8] and $KGdF_4$ [10] transform directly into the cubic phases and the trigonal polymorphs are not detected. Recently, Park[19] has observed an irreversible pressure-induced phase transition in trigonal $KY_{0.9}Er_{0.1}F_4$ above 5 GPa using photoluminescence. The high-pressure phase is argued to have a smaller unit cell and higher symmetry with respect to the one at atmospheric pressure.

When doped with other rare earths, cubic KMF_4 (M = Y, rare earth) and trigonal KYF_4 are highly efficient phosphors.[10–27] KYF_4 is considered as a host for solid state lasers and as a thermo-luminescent material for radiation detectors and dosimeters. What makes this compound especially attractive is its multisite structure.[20–27] It is superior to many other compounds in terms of up-conversion luminescence efficiency due to the interactions of dopant ions located at various lattice sites. According to some earlier studies, luminescence data on doped trigonal KYF_4 cannot be

[a]*Institute of Crystallography, RWTH Aachen, 52066 Aachen, Germany. E-mail: grzechnik@xtal.rwth-aachen.de*
[b]*Kurnakov Institute of General and Inorganic Chemistry, 119991 Moscow, Russia*
[c]*Jülich Centre for Neutron Science, 52425 Jülich, Germany*

†Electronic supplementary information (ESI) available. CCDC 891236–891242. For ESI and crystallographic data in CIF or other electronic format see DOI: 10.1039/c2dt31483e

Published on 19 October 2012 on http://pubs.rsc.org | doi:10.1039/C2DT31483E
Downloaded by Forschungszentrum Julich GmbH on 08/05/2013 08:19:34.

exclusively interpreted on the basis of a fully ordered K–Y distribution in the lattice so that it was assumed that some of the sites are occupied by both Y and K.[20,23,25] Lanthanide-doped $KGdF_4$ nanocrystals are considered to be multifunctional as they are both paramagnetic and up-converting materials useful for bimodal bio-probes.[14,28]

We are generally interested in the crystal structures and stabilities of the AMF_4 materials (A = Li, Na, K; M = Y, rare earth) that are related to the fluorite structure with various schemes of cation (dis)ordering.[29–34] A series of studies at various conditions has previously been carried out on KY_3F_{10} that is a related material to KYF_4 in the system KF–YF_3. At ambient pressure and room temperature, it is an anion-excess $2 \times 2 \times 2$ superstructure of fluorite in space group $Fm\bar{3}m$, a = 11.553(1) Å.[35] At high temperatures and high pressures, it converts to another fluorite superstructure (space group $Pm\bar{3}m$, $a \approx 5.7$ Å) with partially disordered fluorine atoms.[36] High-temperature mobility of the F atoms in the $2 \times 2 \times 2$ superstructure was investigated with X-ray diffraction at atmospheric pressure by Friese *et al.*[37]

In this work, we use synchrotron radiation to re-examine the crystal structure of KYF_4 in view of the inconsistencies between the structural models[1–4] and some spectroscopic data, in which space group $P3_112$ was assumed but not confirmed with the X-ray data.[25] In addition, the structures of the $KLnF_4$ materials with heavier lanthanides (Ln = Ho, Er, Tm) and $KYbF_4$ doped with Er^{3+} are solved. Based on the measurements in diamond anvil cells, we determine the high-pressure stability of KYF_4 and Er:$KYbF_4$.

Experimental

Single crystals of pure KYF_4, $KHoF_4$, $KErF_4$, $KTmF_4$, and Er:$KYbF_4$ were grown using the hydrothermal method.[2,38] The Er doping in $KYbF_4$ is 1.0 at%.

A polycrystalline sample of KYF_4, prepared by grinding some of the single crystals, was studied at atmospheric pressure with X-ray powder diffraction at the ANKA Synchrotron Light Source in Karlsruhe. The room-temperature data were collected on the *PDIFF* beamline with the Bragg–Brentano geometry (λ = 0.6498 Å, the angular step of 0.004°). The low-temperature data were measured on the IPDS-2 diffractometer at the *SCD* beamline (λ = 0.8000 Å) using capillaries and the Cryostream 700 N_2 device (Oxford Cryosystems).

The experiments on single-crystals at ambient and high pressures (λ = 0.4000 Å) were performed at room temperature on the beamline *D*3 at HASYLAB (Hamburg) equipped with a HUBER four-circle diffractometer and a marCCD165 detector. The high-pressure single-crystal data were collected in the Ahsbahs[39] and Boehler-Almax[40] diamond anvil cells at room temperature. A 4 : 1 mixture of methanol and ethanol was used as the pressure medium and the ruby luminescence method[41] was used for pressure calibration.

For all the synchrotron single-crystal measurements, the intensities were indexed and integrated using the program XDS.[42] Further treatment of the high-pressure single-crystal data was carried out according to the procedures described by Friese *et al.*[43] and Posse *et al.*[44] Structure refinements were carried out with the program Jana2006.[45] All the relevant experimental, structural, and geometrical details are given below and in the ESI.†

Results and discussion

The powder pattern of KYF_4 at ambient pressure and room temperature could be indexed[46] with a trigonal lattice a = 14.16 Å and c = 10.19 Å with the figures of merit $M(20)$ = 176.7 and $F(20)$ = 621.6 (0.0007, 49). No phase transition is detected at low temperatures down to 100 K (Fig. 1). The c lattice parameter is essentially insensitive to the temperature changes. The temperature dependence of the lattice parameters is fitted with the polynomial functions $a = 14.1012 - 4.22471 \times 10^{-5}\ T + 8.28432 \times 10^{-7}\ T^2$ and $c = 10.18524 + 1.67343 \times 10^{-5}\ T$.

All reflections in the single-crystal diffraction patterns of all the compounds at ambient pressure can be indexed with a trigonal cell $a \approx 14$ Å and $c \approx 10$ Å. The observed extinction rules $00l$: $l = 3n$ are in accordance with enantiomorphic space groups $P3_1$ and $P3_2$. Refinements of the data in space group $P3_1$ were started from the model in ref. 1. For the refinements in space group $P3_2$, the corresponding starting coordinates were deduced from the model in $P3_1$.[1] It has to be noted that the refinements of the data for KYF_4, $KTmF_4$, and Er:$KYbF_4$ in space group $P3_1$ did not converge. Hence, our structural work clearly indicates that the compounds $KHoF_4$ and $KErF_4$ crystallize in space group $P3_1$, while the other three compounds with Ln = Tm, Yb or Y crystallize in space group $P3_2$ (Table 1 and Fig. 2). It is interesting in this context to note that in former structure determinations on KYF_4 and $KY_{0.95}Er_{0.05}F_4$ from the laboratory data[1,2] the space group was found to be $P3_1$.

An additional twin operation corresponding to a 2-fold rotation around the [120] direction had to be taken into

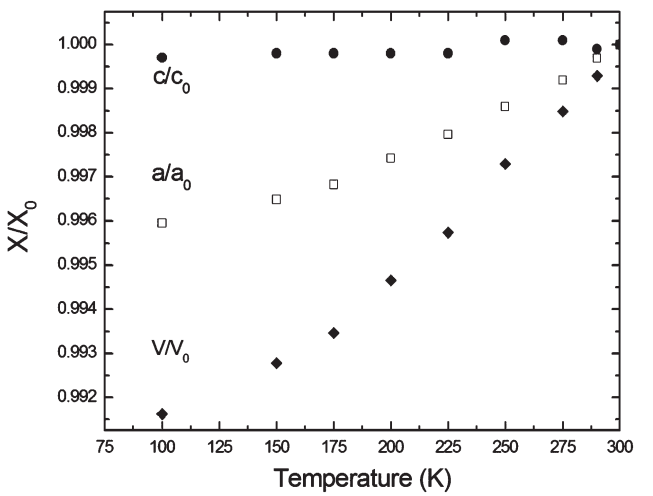

Fig. 1 Temperature dependence of normalized lattice parameters and unit-cell volumes of KYF_4 at ambient pressure.

This journal is © The Royal Society of Chemistry 2013

Downloaded by Forschungszentrum Julich Gmbh on 08/05/2013 08:19:34.
Published on 19 October 2012 on http://pubs.rsc.org | doi:10.1039/C2DT31483E

Table 1 Experimental details for $KLnF_4$ at ambient pressure. The single-crystal data were collected at HASYLAB. The powder data to determine the lattice parameters for KYF_4 were measured at ANKA

Material	$KHoF_4$	$KErF_4$	$KTmF_4$	Er:$KYbF_4$	KYF_4
Crystal data					
Space group	$P3_1$	$P3_1$	$P3_2$	$P3_2$	$P3_2$
a (Å)	14.190(1)	14.128(2)	14.087(2)	14.026(2)	14.163(1)
c (Å)	10.200(1)	10.158(1)	10.146(1)	10.119(1	10.190(1)
V (Å^3)	1778.7	1755.9	1743.7	1726.0	1770.2
ρ (g cm^{-3})	4.704	4.805	4.867	4.994	3.443
λ (Å)	0.4000	0.4000	0.4000	0.4000	0.4000
μ (mm^{-1})	4.583	4.832	5.241	5.598	3.500
G_{iso}	0.60(2)	0.29(2)	0.52(4)	0.052(6)	1.14(6)
Data collection					
No. measured refl.	100 915	113 899	100 309	100 600	138 252
No. observed refl.[a]	23 386	21 805	24 254	17 614	23 443
h_{min},h_{max}	−30,30	−30,30	−30,29	−30,30	−31,31
k_{min},k_{max}	−30,30	−30,30	−30,30	−30,30	−30,30
l_{min},l_{max}	−22.22	−21.21	−22,22	−21,22	−22,21
$R(int)_{obs/all}$ [b]	5.24/5.32	6.71/6.92	4.12/4.13	6.81/7.39	4.73/4.90
Refinement					
$R_{obs/all}$	3.04/3.44	3.12/3.86	3.01/3.10	3.81/5.87	3.06/3.61
w$R_{obs/all}$	3.50/3.58	7.50/7.80	3.85/3.86	3.53/3.84	4.00/4.09
$GoF_{obs/all}$	1.19/1.21	1.05/1.08	1.71/1.73	1.09/1.18	1.19/1.21
No. parameters	231	229	231	231	231

[a] The criterion for observed reflections is $|F_{obs}| > 3\sigma$. [b] All agreement factors are given in %; weighting scheme $1/[\sigma^2(F_{obs}) + (0.01F_{obs})^2]$.

account in all the refinements. The introduction of this twin operation led to lowering of the overall agreement factors by more than 2% in all cases. The refined twin volume fractions for both individuals are close to 0.5 : 0.5 in all refinements. The introduction of further twin domains corresponding to twinning by merohedry type I or II led neither to an improvement of the overall agreement factors nor to significant volume fractions of the additional twin individuals and was therefore discarded. These additional twin refinements clearly show that all the measured crystals are composed of one enantiomorph only.

Close inspection of the refined structures revealed that groups of three atoms of the same type were related *via* a pseudo-centring operation X = (0,0,0), (1/3,2/3,0), (2/3,1/3,0). This caused correlations in the refinement and large errors in the refined atomic parameters, in particular in the displacement parameters. A series of restrictions was thus introduced and the displacement parameters of the fluorine ions, related *via* the pseudo-centring operations, were set equal. The introduction of these restrictions did not lead to significantly higher agreement factors, while, on the other hand, it reduced the errors of the atomic parameters considerably.

Refinements of the high-pressure single-crystal data were carried out accordingly. In this case, however, the restrictions resulting from the pseudo-centring operations were also applied to all the cations. Fluorine ions in the high-pressure structures were only refined isotropically.

For all the compounds at all pressures, trial refinements were performed, in which mixed occupancies of the potassium and trivalent ions were assumed at the cationic sites. However, no significant deviations from the ideal ordered distributions of the two cations could be observed.

The crystal structures for the $KLnF_4$ compounds determined here in the two enantiomorphic space groups $P3_1$ and $P3_2$ are essentially isotypic to the KYF_4 structure determined earlier by Le Fur *et al.*,[1,2] in which the cations are distributed in three layers perpendicular to the c axis (Fig. 2 and 3). Each of these layers is built of two [LnF_7] pentagonal bipyramids alternating with chains of edge-shared distorted [KF_8] cubes. The pseudo-centring operations discussed earlier imply that the six coordination polyhedra around the Ln^{3+} ions in $KLnF_4$ can be divided into two groups of three each, (group 1: $Ln1F_7$, $Ln3F_7$, $Ln5F_7$) and (group 2: $Ln2F_7$, $Ln4F_7$, $Ln6F_7$), respectively (Table 2). In each compound, the average Ln–F distances in all six LnF_7 polyhedra are basically the same. However, polyhedra belonging to group 1 are slightly smaller by approximately 3% than polyhedra belonging to group 2. In addition, polyhedral distortions are similar for each group of three individual LnF_7 polyhedra related by the pseudo-centring operations, yet considerably different between the two groups.

Er:$KYbF_4$ and KYF_4 were studied at high pressures using synchrotron single-crystal diffraction in diamond anvil cells. Both of them undergo irreversible pressure-induced phase transitions above about 4 GPa. In each case, they become fragmented into several crystallites (as observed under a microscope) indicating the first-order type of the transformations. The data for KYF_4 collected at 4.12 GPa could tentatively be indexed with the primitive hexagonal lattice $a \approx 16.1$ Å and $c \approx 19.6$ Å. Unfortunately, it was not possible to reliably integrate the data and to subsequently determine the high-pressure structure. Hence, our data measured above the phase transition neither support nor contradict the statement by Park[19] that the high-pressure phase of related $KY_{0.9}Er_{0.1}F_4$

Downloaded by Forschungszentrum Julich Gmbh on 08/05/2013 08:19:34.
Published on 19 October 2012 on http://pubs.rsc.org | doi:10.1039/C2DT31483E

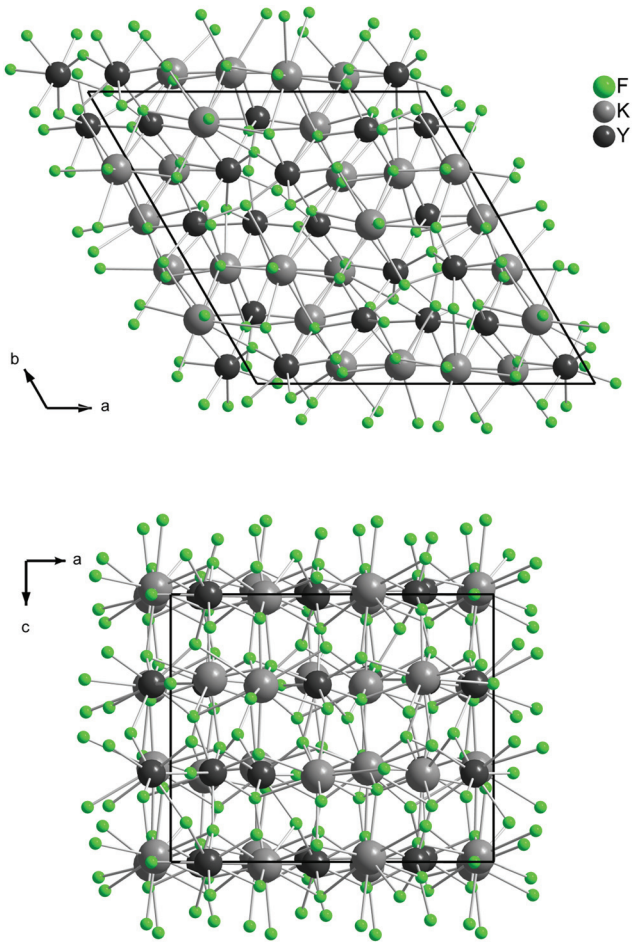

Fig. 2 Crystal structure of KYF_4 (space group $P3_2$) at ambient pressure.

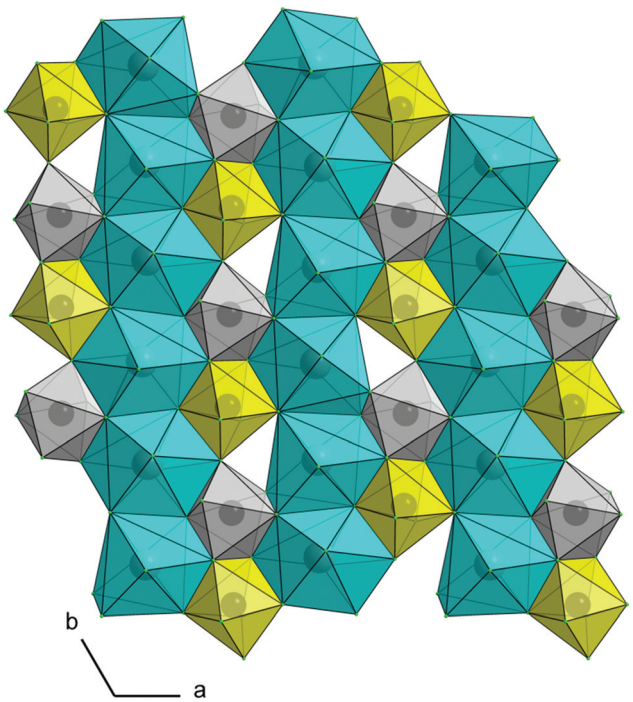

Fig. 3 Polyhedral representation of one layer in the structure of KYF_4 (space group $P3_2$) at ambient pressure. YF_7-polyhedra belonging to groups 1 and 2 are in yellow and grey, respectively. KF_8 polyhedra are shown in cyan.

Table 2 Selected average distances and geometrical parameters (all in Å) in the structure of $KLnF_4$ at ambient conditions

<Ho1–F>	2.25	<Ho3–F>	2.24	<Ho5–F>	2.25
Range Ho1–F	0.14	Range Ho3–F	0.14	Range Ho5–F	0.15
<Ho2–F>	2.25	<Ho4–F>	2.25	<Ho6–F>	2.25
Range Ho2–F	0.06	Range Ho4–F	0.07	Range Ho6–F	0.07
<Er1–F>	2.24	<Er3–F>	2.24	<Er5–F>	2.24
Range Er1–F	0.15	Range Er3–F	0.14	Range Er5–F	0.15
<Er2–F>	2.24	<Er4–F>	2.24	<Er6–F>	2.24
Range Er2–F	0.06	Range E4r–F	0.07	Range Er6–F	0.06
<Tm1–F>	2.23	<Tm3–F>	2.23	<Tm5–F>	2.22
Range Tm1–F	0.15	Range Tm3–F	0.15	range Tm5–F	0.15
<Tm2–F>	2.24	<Tm4–F>	2.23	<Tm6–F>	2.23
Range Tm2–F	0.06	Range Tm4–F	0.08	Range Tm6–F	0.07
<Yb1–F>	2.21	<Yb3–F>	2.21	<Yb5–F>	2.22
Range Yb1–F	0.18	Range Yb3–F	0.19	Range Yb5–F	0.20
<Yb2–F>	2.22	<Yb4–F>	2.23	<Yb6–F>	2.21
Range Yb2–F	0.11	Range Yb4–F	0.12	Range Yb6–F	0.08
<Y1–F>	2.24	<Y3–F>	2.24	<Y5–F>	2.24
Range Y1–F	0.14	Range Y3–F	0.15	Range Y5–F	0.14
<Y2–F>	2.25	<Y4–F>	2.24	<Y6–F>	2.24
Range Y2–F	0.08	Range Y4–F	0.08	Range Y6–F	0.07

should have higher symmetry. On the other hand, the large unit cell that we determine for KYF_4 might arise from breaking of the crystal.

Up to 4 GPa, Er:$KYbF_4$ and KYF_4 are more compressible along the c axis (Tables 1, 3 and 5). Their bulk compressibility predominantly results from the contraction of the KF_8 polyhedra (Tables 2, 4 and 6). There is no significant effect of high pressure on the distortions of the coordination spheres around the trivalent cations as seen from the comparison of the ranges of the Yb–F and Y–F distances, respectively.

Since the structures of the $KLnF_4$ compounds are related to the structure of CaF_2 (space group $Fm\bar{3}m$)[1–4] they can be analysed with respect to their pseudo-symmetry. Fig. 4 shows a diagram illustrating the group–subgroup relationship between the ideal fluorite structure and the trigonal superstructures of $KLnF_4$ in space group $P3_1$. For the compounds crystallizing in space group $P3_2$, the relationships are similar and can be deduced by replacing each of the space groups in the diagram by the enantiomorphic group. The lattice of fluorite can be related to the lattice of the $KLnF_4$ compounds through the equations $a_F = -a + 2b - c$, $b_F = -a - b + 2c$, $c_F = a + b + c$.

To quantify the degree of pseudo-symmetry, the program PSEUDO was used.[47]‡ Using the atomic coordinates given in the ESI,† one can deduce that the pseudo-symmetry of the

‡The measure of pseudo-symmetry is the maximum atomic displacement between the atomic site in the low-symmetry structure and the site in the high-symmetry structure. As the two minimal supergroups in this case have different indices ($t = 2$ for $P3_112$ and $P3_212$ and $k = 3$ for $P3_1$ and $P3_2$), this maximum distance is used as the measure in the following discussion.

This journal is © The Royal Society of Chemistry 2013

Downloaded by Forschungszentrum Julich GmbH on 08/05/2013 08:19:34.
Published on 19 October 2012 on http://pubs.rsc.org | doi:10.1039/C2DT31483E

Table 3 Experimental details for Er:$KYbF_4$ at 3.98 GPa. The data were collected at HASYLAB

Crystal data	
Space group	$P3_2$
a (Å)	13.754(3)
c (Å)	9.891(2)
V (Å^3)	1620.4
ρ (g cm^{-3})	5.313
λ (Å)	0.4000
μ (mm^{-1})	5.956
G_{iso}	0.14(3)
Data collection	
No. measured refl.	25 800
No. observed refl.[a]	9785
h_{min},h_{max}	−25, 26
k_{min},k_{max}	−26, 24
l_{min},l_{max}	−18, 11
$R(int)_{obs/all}$ [b]	9.17/9.17
Refinement	
$R_{obs/all}$	8.28/8.28
w$R_{obs/all}$	8.62/8.62
GoF$_{obs/all}$	3.81/3.81
No. parameters	143

[a] The criterion for observed reflections is $|F_{obs}| > 3\sigma$. [b] All agreement factors are given in %; weighting scheme $1/[\sigma^2(F_{obs}) + (0.01F_{obs})^2]$.

Table 4 Selected average distances and geometrical parameters (all in Å) in the structure of Er:$KYbF_4$ at 3.98 GPa

<Yb1–F>	2.20	<Yb3–F>	2.19	<Yb5–F>	2.18
Range Yb1–F	0.21	Range Yb3–F	0.12	Range Yb5–F	0.14
<Yb2–F>	2.20	<Yb4–F>	2.19	<Yb6–F>	2.20
Range Yb2–F	0.11	Range Yb4–F	0.07	Range Yb6–F	0.13

Table 5 Experimental details for KYF_4 at high pressures. The data at 2.04 GPa were collected at HASYLAB

Pressure (GPa)	2.04
Crystal data	
Space group	$P3_2$
a (Å)	14.006(2)
c (Å)	10.062(1)
V (Å^3)	1709.4
ρ (g cm^{-3})	3.5658
λ (Å)	0.4000
μ (mm^{-1})	3.624
G_{iso}	0
Data collection	
No. measured refl.	17 909
No. observed refl.[a]	8379
h_{min},h_{max}	−21, 26
k_{min},k_{max}	−26, 26
l_{min},l_{max}	−16, 17
$R(int)_{obs/all}$ [b]	9.67/9.67
Refinement	
$R_{obs/all}$	7.30/7.30
w$R_{obs/all}$	7.24/7.24
GoF$_{obs/all}$	2.67/2.67
No. parameters	142

[a] The criterion for observed reflections is $|F_{obs}| > 3\sigma$. [b] All agreement factors are given in %; weighting scheme $1/[\sigma^2(F_{obs}) + (0.01F_{obs})^2]$.

Table 6 Selected average distances and geometrical parameters (all in Å) in the structure of KYF_4 at 2.04 GPa

<Y1–F>	2.23	<Y3–F>	2.23	<Y5–F>	2.24
Range Y1–F	0.19	Range Y3–F	0.12	Range Y5–F	0.17
<Y2–F>	2.23	<Y4–F>	2.23	<Y6–F>	2.23
Range Y2–F	0.08	Range Y4–F	0.07	Range Y6–F	0.07

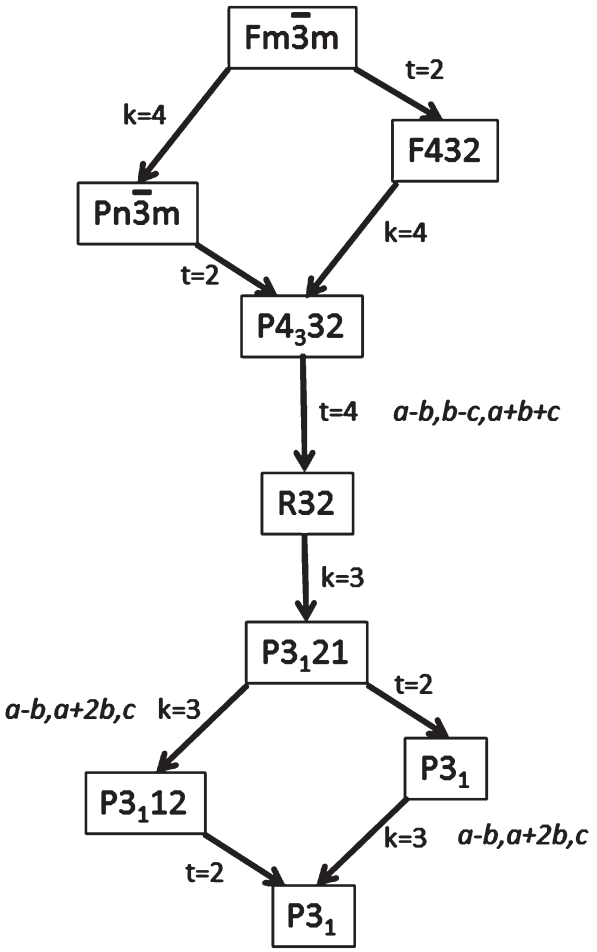

Fig. 4 Group–subgroup relationships involved in the symmetry reduction from the archetype fluorite structure to the structure of $KLnF_4$ in space group $P3_1$.

$KLnF_4$ structures with respect to the minimal $k = 3$ supergroup and the minimal $t = 2$ supergroup involves only small displacements of the atoms. In all these structures, there is a completely ordered distribution of the cations. An increase of the (pseudo)symmetry to $R32$ is only possible if one assumes a disorder of K^+ and Ln^{3+}. However, we found no indication of the cationic disorder in any of the structures investigated here. It is noticeable that the pseudo-symmetry of the structures (Fig. 5) with respect to the two minimal supergroups $k = 3$ and $t = 2$ increases with decreasing radius of the Ln^{3+} cation. The high pseudo-symmetry with respect to the $t = 2$ supergroups is also reflected in the fact that the 2-fold rotation around the [120] direction had to be taken into account in all the structural refinements.

Downloaded by Forschungszentrum Julich Gmbh on 08/05/2013 08:19:34.
Published on 19 October 2012 on http://pubs.rsc.org | doi:10.1039/C2DT31483E

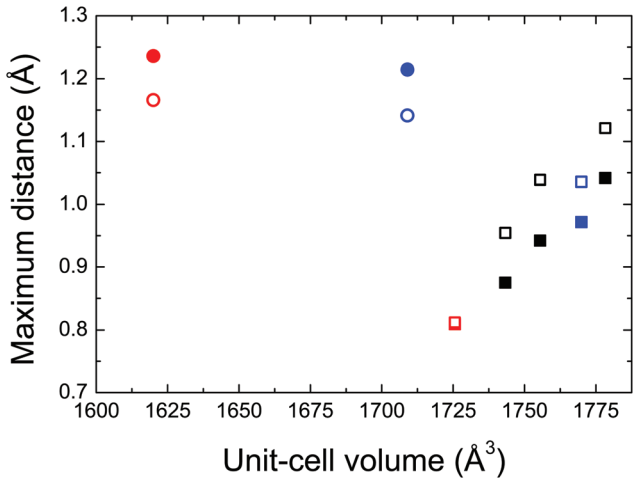

Fig. 5 Maximum distances between the original atomic positions and the symmetry related positions in the hypothetical higher-symmetry structures for the $KLnF_4$ compounds at ambient conditions (squares) and upon compression (circles) as a function of the unit-cell volumes. The full symbols stand for the t = 2 minimal supergroups ($P3_112$ and $P3_212$), while the open symbols stand for the k = 3 minimal supergroups ($P3_1$ and $P3_2$). The red and blue symbols represent the data for Er:$KYbF_4$ and KYF_4, respectively.

It should be noted that the hypothetical superstructure of the $KLnF_4$ compounds with space group $P3_1$ obtained through the transformation k = 3 (Fig. 4) is closely related to that of $KTlF_4$.[1,48] The pseudo-centring operations relating three individual atoms in the structures of the $KLnF_4$ compounds, which were taken into account in the refinements (see above), correspond to this $KTlF_4$ superstructure type, *i.e.*, to the underlying pseudo-symmetry with respect to the minimal k = 3 subgroup (Fig. 4).

According to Abrahams,[3,4] KYF_4 fulfills all the criteria to be a potential ferroelectric material and our analysis of the pseudo-symmetry shows that the same is true for all the other $KLnF_4$ compounds at atmospheric conditions. At high pressures, the pseudo-symmetry in Er:$KYbF_4$ and KYF_4 is decreased and larger displacements of the atoms are necessary to reach the higher symmetrical space group $P3_221$ (Fig. 5).

Conclusions

The results of our work using synchrotron single-crystal and powder diffraction indicate that $KHoF_4$ and $KErF_4$ crystallize in space group $P3_1$, while $KTmF_4$, Er:$KYbF_4$, and KYF_4 crystallize in space group $P3_2$. An analysis of the ambient-pressure crystal structures with respect to the minimal supergroups $P3_112$ and $P3_212$ (t = 2) shows that their pseudo-symmetry increases with decreasing radius of the Ln^{3+} ion. It is also reflected in the fact that all the investigated crystals are twinned with the additional 2-fold axis as a twinning operation. In addition, pseudo-symmetry with respect to the minimal supergroups $P3_1$ and $P3_2$ (k = 3) gives rise to a pseudo-centring X = (0,0,0), (1/3,2/3,0), (2/3,1/3,0). Pseudo-symmetry with respect to this minimal k-supergroup also increases with decreasing radius of Ln^{3+}. At high pressures, pseudo-symmetry in Er:$KYbF_4$ and KYF_4 is decreased and larger displacements of the atoms are necessary to reach the higher symmetrical space groups t = 2 and k = 3. While external pressure induces first-order phase transitions in Er:$KYbF_4$ and KYF_4 above 4 GPa, it has no effect on the distribution of the cations in their structures at lower pressures.

The crystal structures determined here from the single crystals grown hydrothermally all exhibit twinning and complete order of the cations. We do not find any evidence for some of the sites being occupied by both Ln and K, like it was observed using optical methods on the KYF_4 crystals grown with the Czochralski method in ref. 20, 23 and 25, in which no diffraction data were shown, although space group $P3_112$, incompatible with our present results, was assumed.[25] Hence, further X-ray diffraction studies on single crystals of the trigonal $KLnF_4$ materials synthesized with other methods than the hydrothermal growth would clarify whether twinning and the (dis)order of the cations might indeed be dependent on the synthetic strategy.

Acknowledgements

Portions of this research were carried out at the light source DORIS III at DESY that is a member of the Helmholtz Association. The research leading to these results has received funding from the European Community's Seventh Framework Programme (FP7/2007–2013) under grant agreement no. 226716.

References

1 Y. Le Fur, N. M. Khaidukov and S. Aléonard, *Acta Crystallogr., Sect C: Cryst. Struct. Commun.*, 1992, **48**, 978.
2 Y. Le Fur, N. M. Khaidukov and S. Aléonard, *Acta Crystallogr., Sect C: Cryst. Struct. Commun.*, 1992, **48**, 2062.
3 S. C. Abrahams, *Acta Crystallogr., Sect B: Struct. Sci.*, 2003, **59**, 541.
4 S. C. Abrahams, *Acta Crystallogr., Sect B: Struct. Sci.*, 2003, **59**, 811.
5 W. H. Zachariasen, *Acta Crystallogr.*, 1949, **2**, 388.
6 W. H. Zachariasen, *J. Am. Chem. Soc.*, 1948, **70**, 2147.
7 W. H. Zachariasen, *Acta Crystallogr.*, 1948, **1**, 265.
8 G. Brunton, *Acta Crystallogr., Sect B: Struct. Sci.*, 1969, **25**, 600.
9 F. Werner, M. Weil and F. Kubel, *Acta Crystallogr., Sect E: Struct. Rep. Online*, 2003, **59**, i47.
10 M. Karbowiak, A. Mech, A. Bednarkiewicz and W. Stręk, *J. Alloys Compd.*, 2004, **380**, 321.
11 M. Karbowiak, A. Mech, L. Kępinski, W. Mielcarek and S. Hubert, *J. Alloys Compd.*, 2005, **400**, 67.
12 H. Schäfer, P. Ptacek, O. Zerzouf and M. Haase, *Adv. Funct. Mater.*, 2008, **18**, 2913.

 This journal is © The Royal Society of Chemistry 2013

Downloaded by Forschungszentrum Julich Gmbh on 08/05/2013 08:19:34.
Published on 19 October 2012 on http://pubs.rsc.org | doi:10.1039/C2DT31483E

13 H. Schäfer, P. Ptacek, K. Hickmann, M. Prinz, M. Neumann and M. Haase, *Russ. J. Inorg. Chem.*, 2009, **54**, 1914.
14 L. W. Yang, Y. Y. Zhang, J. J. Li, J. X. Zhong and P. K. Chu, *Nanoscale*, 2010, **2**, 2805.
15 N. Tyagi, A. A. Reddy and R. Nagarajan, *Opt. Mater.*, 2010, **33**, 42.
16 M. Haase and H. Schäfer, *Angew. Chem., Int. Ed.*, 2011, **50**, 5808.
17 Y. H. Wang, Y. S. Liu, Q. B. Xiao, H. M. Zhu, R. F. Li and X. Y. Chen, *Nanoscale*, 2011, **3**, 3164.
18 S. Das, A. A. Reddy, S. Ahmad, R. Nagarajan and G. V. Prakash, *Chem. Phys. Lett.*, 2011, **508**, 117.
19 T.-R. Park, *J. Korean Phys. Soc.*, 2012, **60**, 812.
20 E. Sani, A. Toncelli, M. Tonelli and F. Traverso, *J. Phys.: Condens. Matter*, 2004, **16**, 241.
21 T.-R. Park, T. Y. Park, S. H. Youn and N. M. Khaidukov, *J. Lumin.*, 2004, **106**, 281.
22 H. W. Kui, D. Lo, Y. C. Tsang, N. M. Khaidukov and V. N. Makhov, *J. Lumin.*., 2006, **117**, 29.
23 E. Sani, A. Toncelli and M. Tonelli, *J. Phys.: Condens. Matter*, 2006, **18**, 2057.
24 L. Bonelli, A. Toncelli, A. Di Lieto and M. Tonelli, *J. Phys. Chem. Solids*, 2007, **68**, 2381.
25 N. Coluccelli, G. Galzerano, L. Bonelli, A. Toncelli, A. Di Lieto, M. Tonelli and P. Laporta, *Appl. Phys. B*, 2008, **92**, 519.
26 E. M. Maddock, R. A. Jackson and M. E. G. Valerio, *J. Phys.: Conf. Series*, 2010, **249**, 012040.
27 D. Parisi, S. Veronesi and M. Tonelli, *Opt. Mater.*, 2011, **34**, 410.
28 Q. Ju, D. Tu, Y. Liu, R. Li, H. Zhu, J. Chen, Z. Chen, M. Huang and X. Chen, *J. Am. Chem. Soc.*, 2012, **134**, 1323.
29 A. Grzechnik, K. Syassen, I. Loa, M. Hanfland and J.-Y. Gesland, *Phys. Rev. B: Condens. Matter*, 2002, **65**, 104102.
30 A. Grzechnik, W. A. Crichton, P. Bouvier, V. Dmitriev, H.-P. Weber and J.-Y. Gesland, *J. Phys.: Condens. Matter*, 2004, **16**, 7779.
31 A. Grzechnik, K. Friese, V. Dmitriev, H.-P. Weber, J.-Y. Gesland and W. A. Crichton, *J. Phys.: Condens. Matter*, 2005, **17**, 763.
32 A. Grzechnik, P. Bouvier, M. Mezouar, M. D. Mathews, A. K. Tyagi and J. Köhler, *J. Solid State Chem.*, 2002, **165**, 159.
33 A. Grzechnik, P. Bouvier, W. A. Crichton, L. Farina and J. Köhler, *Solid State Sci.*, 2002, **4**, 895.
34 A. Grzechnik and K. Friese, *Dalton Trans.*, 2012, **41**, 10258.
35 A. Grzechnik, J. Nuss, K. Friese, J.-Y. Gesland and M. Jansen, *Z. Kristallogr.- New Cryst. Struct.*, 2002, **217**, 460.
36 A. Grzechnik, W. A. Crichton and J.-Y. Gesland, *Solid State Sci.*, 2003, **5**, 757.
37 K. Friese, H. Krüger, V. Kahlenberg, T. Balic-Zunic, H. Emerich, J.-Y. Gesland and A. Grzechnik, *J. Phys.: Condens. Matter*, 2006, **18**, 2677.
38 N. M. Khaidukov, P. P. Fedorov and N. A. Abramov, *Neorg. Mater.*, 1991, **27**, 2614.
39 H. Ahsbahs, *Z. Kristallogr.*, 2004, **219**, 305.
40 R. Boehler, *Rev. Sci. Instrum.*, 2006, **77**, 115103.
41 H. K. Mao, J. Xu and P. M. Bell, *J. Geophys. Res.*, 1986, **91**, 4673.
42 W. Kabsch, *Acta Crystallogr. Sect D: Biol. Crystallogr.*, 2010, **66**, 125.
43 K. Friese, Y. Kanke and A. Grzechnik, *Acta Crystallogr., Sect B: Struct. Sci.*, 2009, **65**, 326.
44 J. M. Posse, K. Friese and A. Grzechnik, *J. Phys.: Condens. Matter*, 2011, **23**, 215401.
45 V. Petricek, M. Dusek and L. Palatinus, *JANA2006 – Crystallographic Computing System*, Institute of Physics, Academy of Sciences of the Czech Republic, Praha, 2006.
46 A. Boultif and D. Louer, *J. Appl. Crystallogr.*, 2004, **37**, 724.
47 E. Kroumova, J. M. Perez-Mato and M. I. Aroyo, *J. Appl. Crystallogr.*, 1998, **31**, 646.
48 Ch. Hebecker, *Z. Naturforsch., B: Chem. Sci.*, 1975, **30**, 305.